PRAMANA
— journal of
physics

Vol. 81, No. 5
November 2013
pp. 873–883

Phase transition properties of a cylindrical ferroelectric nanowire

WANG YING[1] and YANG XIONG[1,2*]

[1]College of Science; [2]Institute of Low Dimensional Materials and Technology,
Civil Aviation University of China, Tianjin 300300, China
*Corresponding author. E-mail: x-yang@cauc.edu.cn

MS received 28 March 2013; revised 28 July 2013; accepted 13 August 2013
DOI: 10.1007/s12043-013-0611-7; ***e*Publication:** 16 October 2013

Abstract. Based on the transverse Ising model (TIM) and using the mean-field theory, we investigate the phase transition properties of a cylindrical ferroelectric nanowire. Two different kinds of phase diagrams are constructed. We discuss systematically the effects of exchange interactions and the transverse field parameters on the phase diagrams. Moreover, the cross-over features of the parameters from the ferroelectric dominant phase diagram to the paraelectric dominant phase diagram are determined for the ferroelectric nanowire. In addition, the polarizations of the surface shell and the core are illustrated in detail by modifying the TIM parameters.

Keywords. Ferroelectrics; cylindrical nanowire; phase transitions.

PACS Nos 77.80.B–; 75.10.Hk

1. Introduction

One-dimensional (1D) ferroelectric nanostructures such as nanowires, nanoubes and nanorods have aroused strong interest in the academia and the industry because of their novel physical properties compared to their bulk counterparts and because of their potential applications in nanoscale piezoelectric transducers and actuators, ultrasonic devices and high-density nonvolatile memory devices [1–7]. Finite size and surface effects on the ferroelectric properties of nanowires are reported in [8,9]. These facts motivated us for further investigation on ferroelectric nanowires.

Much of the theoretical work uses the phenomenological Devonshire–Landau–Ginzburg theory and the transverse Ising model for studying ferroelectrics. Tilly and Zěkš [10] first introduced the phenomenological approach to investigate ferroelectric films with a second-order phase transition. The theory was then used by Schwenk and co-workers [11–13] to study the static and dynamic properties of ferroelectric superlattices. Zhong and co-workers [14,15] discussed the size effects of ferroelectric particles. For a

cylindrical ferroelectric nanowire, one problem with the phenomenological theory is that it is not clear how to account for the coupling between shells in a nanowire within a continuum theory. Approaches based on the transverse Ising model have the advantage that the coupling between shells can be automatically described by an inter-shell exchange constant. The transverse Ising model within the framework of the pseudospin theory is successful in describing the phase transition behaviour of hydro-bonded ferroelectrics, such as thin films, superlattices and particles [16–23], since the transition to ferroelectricity is associated with preferential occupation by the protons of one or the other of the two equivalent wells in the hydrogen bonds [24]. Based on the model, Kaneyoshi studied the phase diagrams, magnetizations and susceptibility of nanowires and nanotubes [25–28]. Wang *et al* used the effective-field theory with correlations for studying the dynamic properties of phase diagrams in a cylindrical ferroelectric nanotube [29].

In the mean-field theory, the TIM parameters are an effective coupling constant and an effective tunnelling field. The mean-field expressions is usually used for a qualitative analysis of the system which gives a surprisingly good quantitative agreement with measured data [24]. In the present paper, we apply the mean-field theory to investigate the phase transition properties of a cylindrical ferroelectric nanowire by taking into account two different exchange interactions and two different transverse field parameters in the TIM. The effects of various parameters on the phase diagrams are given, and the crossover features of the parameters for the ferroelectric nanowire are determined. This paper will also show how the polarizations on the surface shell and the core depend on the parameters.

2. The Hamiltonian and method

We consider a cylindrical ferroelectric nanowire, as shown in figure 1. The system consists of one shell on the surface and two shells in the core. In the cross-section of the nanowire, the pseudospins on the surface and second shells compose two regular hexagons respectively. The system can be described by the Ising model in a transverse field and the Hamiltonian of the model is given by [16–18]

$$H = -\sum_i \Omega_i S_i^x - \frac{1}{2}\sum_{ij} J_{ij} S_i^z S_j^z, \tag{1}$$

where Ω_i is the transverse field, S_i^x and S_i^z are the x and z components of a spin-$\frac{1}{2}$ operator at site i and J_{ij} is the exchange interaction constant between the ith and the jth site, where i and j run over only the nearest-neighbouring sites. Ω_s and Ω are different transverse fields on the surface and inside the nanowire. $J_{ij} = J_s$ if sites i, j are located in the surface shell and $J_{ij} = J_s$ if sites i, j are located in the surface shell and the second shell respectively, while $J_{ij} = J_1$ otherwise.

Similar to the magnetic Ising model [25], the pseudospins on the surface shell are located in two different sites. By applying mean-field approximation, the spin averages along the z direction in the two sites, $\langle S_{1a}^z \rangle$ and $\langle S_{1b}^z \rangle$, can be written as [16–18]

$$\langle S_i^z \rangle = \frac{H_i^z}{2\sqrt{\Omega_s^2 + (H_i^z)^2}} \tanh \frac{\sqrt{\Omega_s^2 + (H_i^z)^2}}{2k_B T}, \quad i = 1a,\ 1b, \tag{2}$$

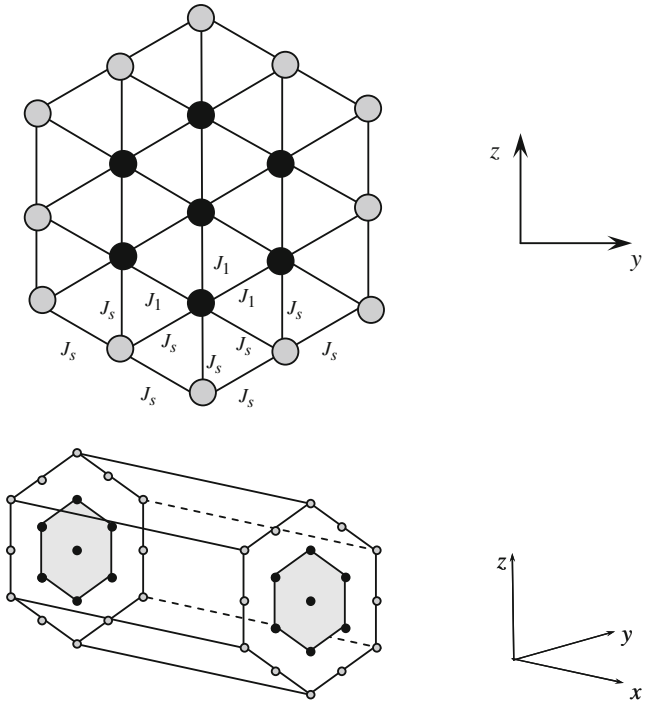

Figure 1. Schematic illustration of a cylindrical ferroelectric nanowire with 2D cross-section and 3D solid. The gray circles represent pseudospins at the surface shell and the black circles are pseudospins constituting the core.

where

$$H_{1a}^z = 2J_s\langle S_{1a}^z\rangle + 2J_s\langle S_{1b}^z\rangle + 2J_s\langle S_2^z\rangle, \tag{3}$$

$$H_{1b}^z = 2J_s\langle S_{1b}^z\rangle + 2J_s\langle S_{1a}^z\rangle + J_s\langle S_2^z\rangle. \tag{4}$$

For the second and the third shells, the pseudospins are assumed to have the same values on the same shell. So we write the spin averages along the z direction, $\langle S_2^z\rangle$ and $\langle S_3^z\rangle$, as follows:

$$\langle S_i^z\rangle = \frac{H_i^z}{2\sqrt{\Omega^2 + (H_i^z)^2}}\ \tanh\frac{\sqrt{\Omega^2 + (H_i^z)^2}}{2k_BT}, \quad i = 2,\ 3, \tag{5}$$

where

$$H_2^z = 4J_1\langle S_2^z\rangle + 2J_s\langle S_{1a}^z\rangle + J_s\langle S_{1b}^z\rangle + J_1\langle S_3^z\rangle, \tag{6}$$

$$H_3^z = 2J_1\langle S_3^z\rangle + 6J_1\langle S_2^z\rangle. \tag{7}$$

Considering that the spin average $\langle S_i^z \rangle$ will be small when the temperature is near the Curie temperature, based on eqs. (2)–(7), we obtain the following linear equations:

$$\tau_s S_{1a} = 2j_s S_{1a} + 2j_s S_{1b} + 2j_s S_2, \tag{8}$$

$$\tau_s S_{1b} = 2j_s S_{1b} + 2j_s S_{1a} + j_s S_2, \tag{9}$$

$$\tau S_2 = 4j_1 S_2 + 2j_s S_{1a} + j_s S_{1b} + j_1 S_3, \tag{10}$$

$$\tau S_3 = 2j_1 S_3 + 6j_1 S_2, \tag{11}$$

where

$$\tau_s = \frac{2\Omega_s}{J} \coth\left(\frac{\Omega_s}{2k_B T}\right), \quad \tau = \frac{2\Omega}{J} \coth\left(\frac{\Omega}{2k_B T}\right)$$

$$j_s = \frac{J_s}{J}, \quad j_1 = \frac{J_1}{J}, \tag{12}$$

and J is a reducing arbitrary parameter. S_i denotes $\langle S_i^z \rangle$.

Based on eqs (9)–(12), the Curie temperature is then determined by the following coefficient determinant:

$$\det \begin{bmatrix} 2j_s - \tau_s & 2j_s & 2j_s & 0 \\ 2j_s & 2j_s - \tau_s & j_s & 0 \\ 2j_s & j_s & 4j_1 - \tau & j_1 \\ 0 & 0 & 6j_1 & 2j_1 - \tau \end{bmatrix} = 0. \tag{13}$$

With the help of eq. (13), the properties of phase transition of the ferroelectric nanowire can be calculated.

Similarly to the treatment to the magnetic Ising model [26], in order to clarify the contributions from the surface shell and the core to the mean polarization, we define the polarization of the surface shell and the core, P_1 and P_2, as follows:

$$P_1 = 2n\mu \frac{\langle S_{1a}^z \rangle + \langle S_{1b}^z \rangle}{2}, \quad P_2 = 2n\mu \frac{6\langle S_2^z \rangle + \langle S_3^z \rangle}{7}, \tag{14}$$

where n is the number of pseudospins in a unit volume and μ is the multiplier relating the dipole moment of the ionic displacement.

3. Results and discussion

In this section, the numerical calculations for the phase diagrams and polarizations of the cylindrical ferroelectric nanowire are presented in the following figures.

The phase diagrams based on the transverse Ising model, such as those for ferroelectric thin films and ferroelectric superlattices, are usually described in two ways: (1) between the Curie temperature and the surface exchange interaction J_s [16–18], (2) between the

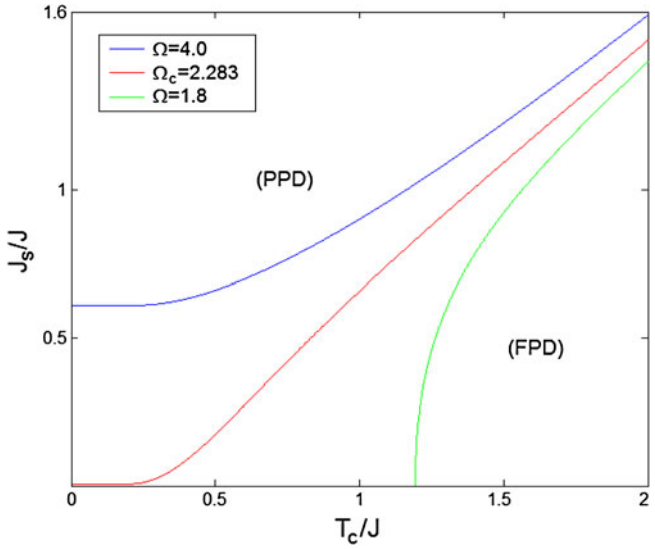

Figure 2. The effect of Ω on the phase diagram J_s vs. T_c. All curves are for $J_1/J = 1.0$ and $\Omega_s/J = 1.5$.

Curie temperature and the surface transverse field Ω_s [18]. In order to obtain the properties of the phase transition, we follow the definitions of the ferroelectric dominant phase diagram (FPD) and the paraelectric dominant phase diagram (PPD) in refs [11,12] (see e.g., figure 2). Figures 2 and 3 are the phase diagrams between the Curie temperature and

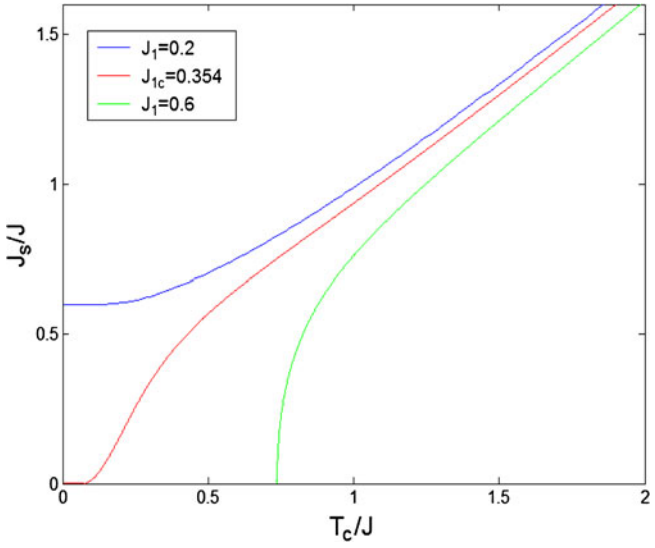

Figure 3. The effect of J_1 on the phase diagram J_s vs. T_c. All curves are for $\Omega/J = 1.0$ and $\Omega_s/J = 2.0$.

the surface exchange interaction for the cylindrical ferroelectric nanowire. Figure 2 gives the effect of the inside transverse field Ω on the phase diagram. Obviously, the curves of J_s vs. T_c depend sensitively on the transverse field Ω. The larger is the parameter Ω, the smaller is the range of ferroelectric phase. The cross-over feature from FPD to PPD can be found in figure 2. It is obvious that when Ω is less than the cross-over value Ω_c, the system is always in FPD, namely, any J_s can result in a transition from ferroelectric to paraelectric phase with increasing temperature. But when Ω is larger than the cross-over value Ω_c, the system is always in PPD, namely, only larger J_s can result in a transition from ferroelectric to paraelectric phase with increasing temperature. Figure 3 shows the effect of inside exchange interaction J_1 on the phase diagram. It indicates that the larger is the parameter J_1, the larger is the range of ferroelectric phase, and there also exists a cross-over value J_{1c} from FPD to PPD. However, the cross-over property of the exchange interaction J_1 is completely opposite to the transverse field Ω. The system is always in FPD when J_1 is larger than the cross-over value J_{1c}, but always in PPD when J_1 is less than J_{1c}. Besides, by comparing figures 2 and 3, it can be concluded that the effect of increasing the transverse field Ω is the same as that of decreasing the exchange interaction J_1.

Figures 4 and 5 are the phase diagram between the Curie temperature and the surface transverse field for the cylindrical ferroelectric nanowire. In figure 4, the dependence of the phase diagram on the inside transverse field Ω can be found. It is obvious that the larger is the parameter Ω, the smaller is the ferroelectric range. This result is consistent with that obtained from figure 2. In figures 5a and 5b, the dependence of the phase diagram on the exchange interaction J_s and J_1 are given. It is noted that the phase diagram depends sensitively on the parameters J_s and J_1. The larger is the parameter J_s or J_1, the

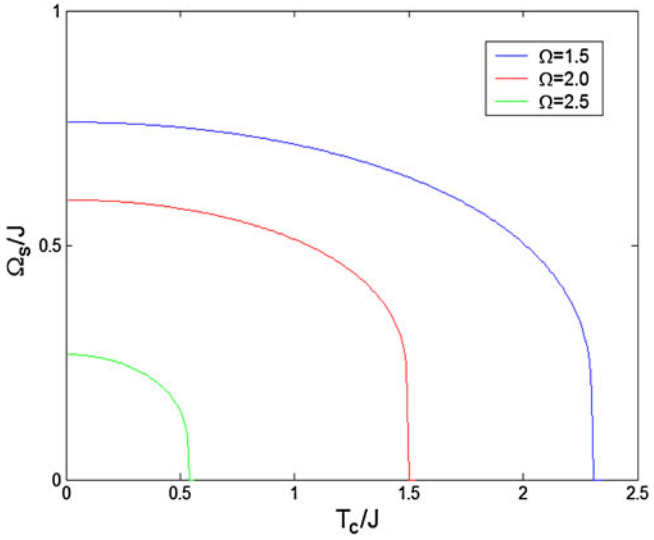

Figure 4. The effect of Ω on the phase diagram Ω_s vs. T_c. All curves are for $J_1/J = 1.0$ and $J_s/J = 1.5$.

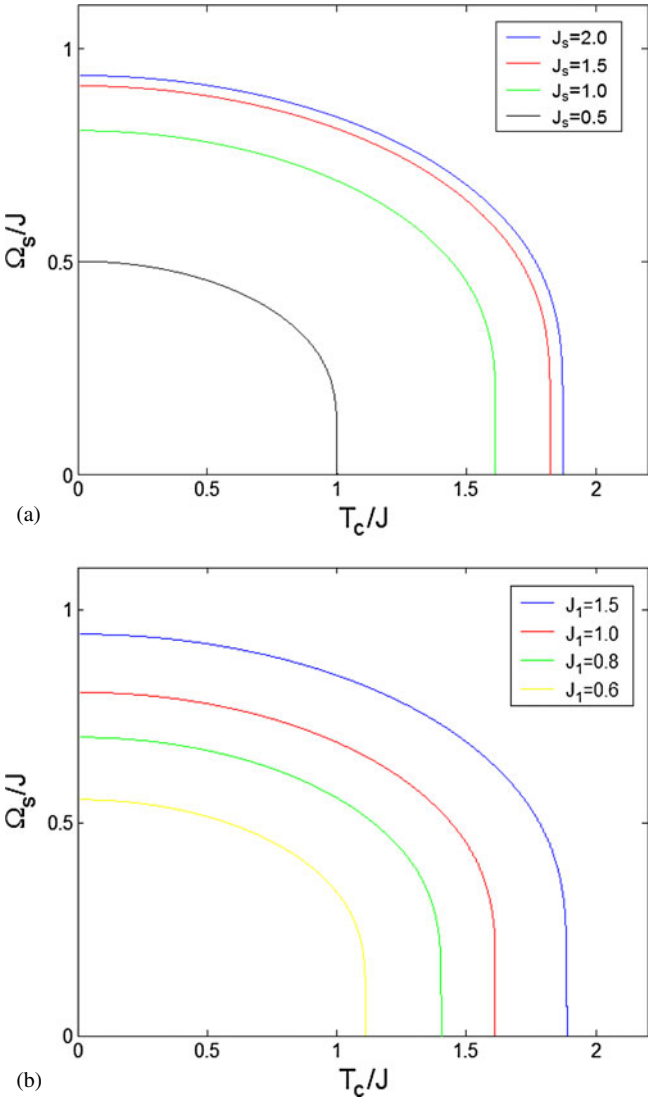

Figure 5. The effects of J_s and J_1 on the phase diagram Ω_s vs. T_c. All curves are for $\Omega = \Omega_s$. (**a**) $J_1/J = 1.0$ and (**b**) $J_s/J = 1.0$.

larger is the range of ferroelectric phase, which is similar to the investigations of the phase diagram in the cylindrical ferroelectric nanotube [29]. Especially, the curves in figures 4 and 5a imply that it is necessary to consider the surface effect in the ferroelectric nanowire by modifying the surface transverse field Ω_s and the surface exchange interaction J_s. In addition, the result from figure 5b is in agreement with that obtained from figure 3.

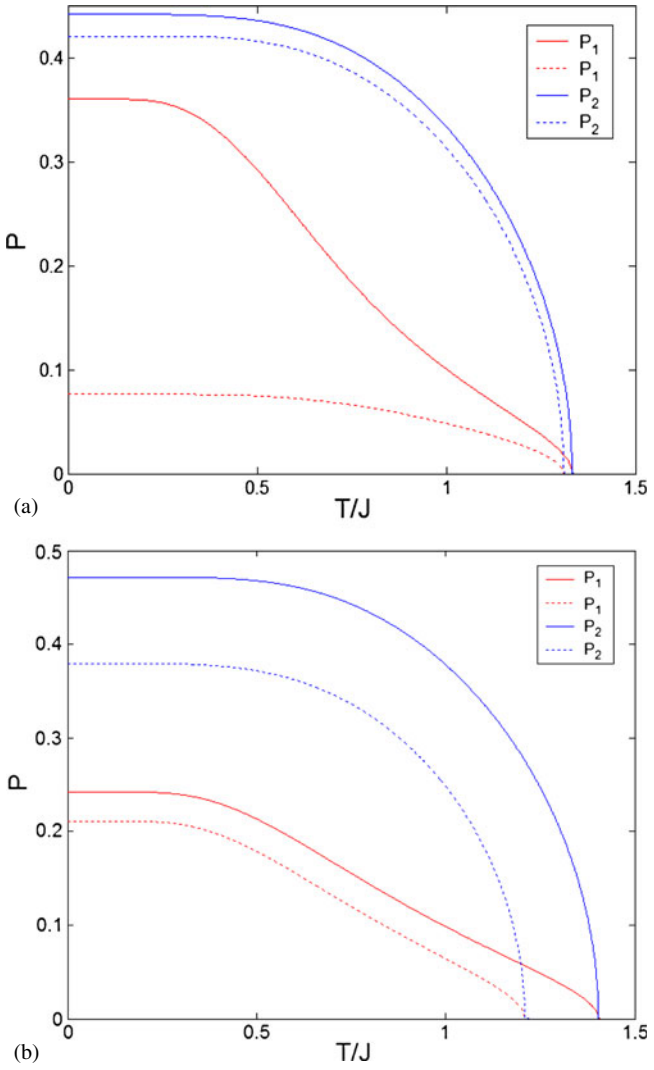

Figure 6. The effects of Ω_s and Ω on the polarizations of the ferroelectric nanowire. All the curves are for $J_s/J = 0.5$ and $J_1/J = 1.0$. (**a**) $\Omega/J = 1.5$, $\Omega_s/J = 1.0$ (solid lines), $\Omega_s/J = 3.0$ (dotted lines) and (**b**) $\Omega_s/J = 1.5$, $\Omega/J = 1.0$ (solid line), $\Omega/J = 2.0$ (dotted lines).

Figures 6 and 7 show the polarizations of the surface shell and the core in the ferroelectric nanowire by considering the modifications of the TIM parameters Ω_s, Ω, J_s and J_1. P_1 and P_2 denote the polarizations of the surface shell and the core. In figures 6 and 7, the curves indicate that the contributions to the mean polarization from the surface shell and the core are completely different below the Curie temperature. It is shown that the polarization P_2 of the core is always larger than the polarization P_1 of the surface shell,

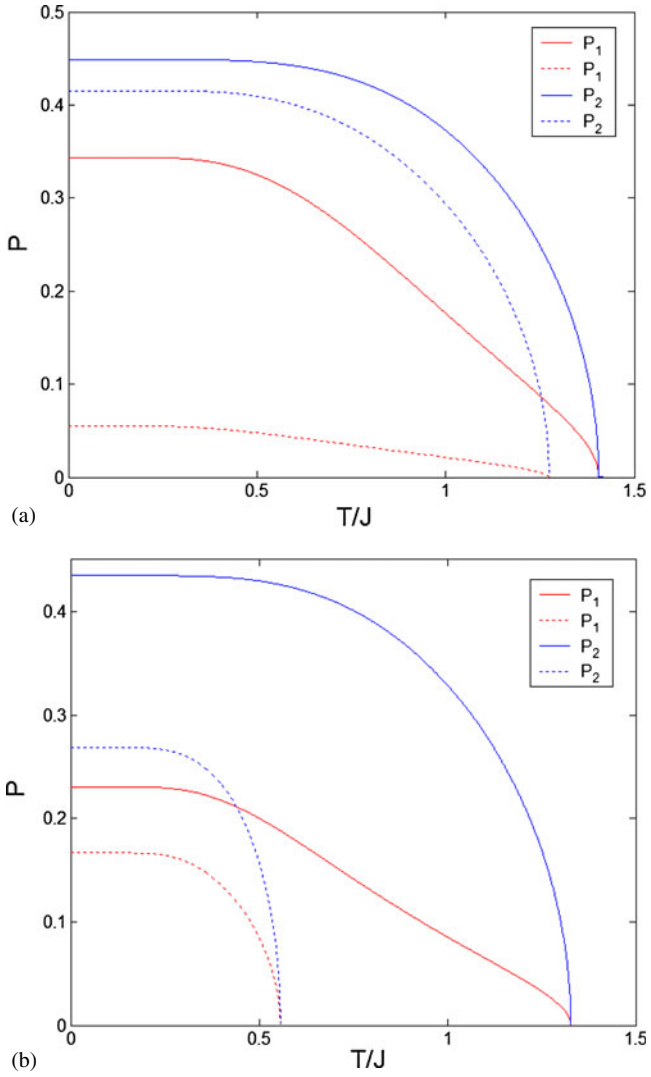

Figure 7. The effects of J_s and J_1 on the polarizations of the ferroelectric nanowire. All the curves are for $\Omega/J = 1.5$ and $\Omega_s/J = 1.5$. (**a**) $J_1/J = 1.0$, $J_s/J = 0.7$ (solid lines), $J_s/J = 0.2$ (dotted lines) and (**b**) $J_s/J = 0.5$, $J_1/J = 1.0$ (solid lines), $J_1/J = 0.5$ (dotted lines).

even though we set the same values of the surface shell parameters J_s and Ω_s with those of the core parameters J_1 and Ω (as shown by the dotted lines in figure 7b). Meanwhile, the figures show how the polarizations depend sensitively on the TIM parameters. The increase of the parameters Ω_s and Ω or the decrease of the parameters J_s and J_1 will result in the decrease of the polarizations P_1 and P_2. The dependences of the polarizations on the surface shell parameters Ω_s and J_s, i.e., the curves in figures 6a and 7a, emphasize the

importance of the surface effect. In figures 6a and 7a, it can be seen that by increasing the surface transverse field Ω_s or decreasing the surface exchange interaction J_s, the surface polarization P_1 decreases more remarkably than the core polarization P_2. In figures 6b and 7b, it can be found that by increasing the inside transverse field Ω or decreasing the inside exchange interaction J_1, the core polarization P_2 decreases more obviously than the surface polarization P_1.

4. Conclusion

In summary, we have studied the phase diagrams and the polarizations of the cylindrical ferroelectric nanowire by taking into account different exchange interactions and different transverse field parameters in the TIM. The phase diagrams and the polarizations depend sensitively on various TIM parameters. The cross-over features for the parameters from FPD to PPD are given for the cylindrical ferroelectric nanowire. In addition, our results show that the phase transition properties of the ferroelectric nanowire are strongly influenced by the surface effects.

Acknowledgements

This work was supported by the Scientific Research Foundation of Civil Aviation University of China (No. 09QD10X), by the Fundamental Research Funds for the Central Universities (ZXH2012N005) and by the 2012 Basic Operational Outlays for the Research Activities of Centric University, Civil Aviation University of China (Grant No. ZXH2012K006).

References

[1] J Junquera and P Ghosez, *Nature* **422**, 506 (2003)
[2] Y Luo, I Szafraniak, N D Zakharov, V Nagarajan, M Steinhart, R B Wehrspohn, J H Wendorff, R Ramesh and M Alexe, *Appl. Phys. Lett.* **83**, 440 (2003)
[3] M W Chu, I Szafraniak, R Scholz, C Harnagea, D Hesse, M Alexe and U Gosele, *Nat. Mater.* **3**, 87 (2004)
[4] A Roelofs, I Schneller, K Szot and R Waser, *Appl. Phys. Lett.* **81**, 5231 (2002)
[5] Y Wang and J J Santiago-Aviles, *Nanotechnol.* **15**, 32 (2004)
[6] J F Scott, F D Morrison, M Miyake and P Zubko, *Ferroelectrics* **336**, 237 (2006)
[7] B J Rodriguez, X S Gao, L F Liu, W Lee, I I Naumov, A M Bratkovsky, D Hesse and M Alexe, *Nano Lett.* **9**, 1127 (2009)
[8] J W Hong and D N Fang, *Appl. Phys. Lett.* **92**, 012906 (2008)
[9] G Pilania, S P Alpay and R Ramprasad, *Phys. Rev. B* **80**, 014113 (2009)
[10] D R Tilly and B Zěkš, *Solid State Commun.* **49**, 823 (1984)
[11] D Schwenk, F Fishman and F Schwabl, *Phys. Rev. B* **38**, 11618 (1988)
[12] D Schwenk, F Fishman and F Schwabl, *Ferroelectrics* **104**, 349 (1990)
[13] D Schwenk, F Fishman and F Schwabl, *J. Phys.: Condense. Matter* **2**, 5409 (1990)
[14] W L Zhong, Y G Wang, P L Zhang and B D Qu, *Phys. Rev. B* **50**, 698 (1994)
[15] Y G Wang, W L Zhong and P L Zhang, *Solid State Commun.* **90**, 329 (1994)

[16] C L Wang, W L Zhong and P L Zhang, *J. Phys.: Condens. Matter* **4**, 4743 (1992)
[17] B H Teng and H K Sy, *Physica B* **348**, 485 (2004)
[18] Baohua Teng and H K Sy, *Phys. Rev. B* **70**, 104115-1 (2004)
[19] A Tabyaoui, A Ainane, B Movaghar and M Saber, *Physica A* **329**, 377 (2003)
[20] B D Qu and P L Zhang, *Ferroelectrics* **197**, 23 (1997)
[21] W L Zhong, *Solid State Commun.* **122**, 311 (2002)
[22] X Yang, Y Wang, C K Wang and Q G Song, *Solid State Commun.* **151**, 1833 (2011)
[23] C L Wang, Y Xin, X S Wang and W L Zhong, *Phys. Rev. B* **62**, 11423 (2000)
[24] R Blinc and B Zeks, *Soft modes in ferroelectrics and antiferroelectrics* (North-Holland, Amsterdam, 1974)
[25] T Kaneyoshi, *J. Magn. Magn. Mater.* **322**, 3014 (2010)
[26] T Kaneyoshi, *J. Magn. Magn. Mater.* **322**, 3410 (2010)
[27] T Kaneyoshi, *J. Magn. Magn. Mater.* **323**, 1145 (2011)
[28] T Kaneyoshi, *Phys. Status Solidi B* **248**, 250 (2011)
[29] C D Wang, Z Z Lu, W X Yuan, S Y Kwok and B H Teng, *Phys. Lett. A* **375**, 3405 (2011)